

Technical Communication

# Thermal and force-chain effects in an experimental, sloping granular shear flow

David Jon Furbish,<sup>1\*</sup> Mark W. Schmeeckle<sup>2</sup> and Joshua J. Roering<sup>3</sup>

<sup>1</sup> Departments of Earth and Environmental Sciences and Civil and Environmental Engineering, Vanderbilt University, Nashville, TN, USA

<sup>2</sup> School of Geographical Sciences, Arizona State University, Tempe, AZ, USA

<sup>3</sup> Department of Geological Sciences, University of Oregon, Eugene, OR, USA

\*Correspondence to: David Jon Furbish, Earth and Environmental Sciences, Vanderbilt University, 2301 Vanderbilt Place, Station B 35-1805, Nashville, Tennessee 37235, USA. E-mail: david.j.furbish@vanderbilt.edu

## Abstract

Force chains figure prominently in shearing motions of granular materials, inasmuch as these chains of load-bearing grains dominate resistance to motion. A simple scaling of the forces involved in the motion of a dry, gravity-driven granular shear flow induced by vibrations (see, e.g., Roering *et al.*, 2001; Roering, 2004) suggests that this shearing motion reflects a balance between the rate of production and the rate of disruption of granular force chains. The rate of production of force chains is proportional to the rate of shear. The rate of disruption is proportional to the rate of shear as force chains ‘age’ during rotation, whence they become unstable and self-destruct. The rate of disruption is also proportional to the frequency and intensity of elastic waves, induced by acoustic vibrations, that propagate through the granular material and weaken force chains. The analysis is empirically consistent with the exponential-like profiles of grain displacement, and the strongly nonlinear increase in grain flux with increasing surface slope, observed in experiments. Copyright © 2008 John Wiley & Sons, Ltd.

**Keywords:** granular flow; force chain; sediment transport

Received 7 September 2007;  
Revised 22 November 2007;  
Accepted 29 November 2007

## Problem

Granular material flows are central to a variety of geomorphic processes, from dry ravel to the migration of sand dunes to the motion of landslides. To inspire thinking about gravity-driven motions of granular material, Roering *et al.* (2001) and Roering (2004) (hereafter referred to as RR) conducted novel experiments in which grains in an acrylic box undergo excitation derived externally from acoustic vibrations (Figure 1), leading to downslope granular flows. In such flows the mean free path of grains is of the same order as the grain diameter (or smaller), and fluctuating grain velocities are of the same order as the local ensemble mean velocity. Campbell (2002) places these flows within an ‘elastic regime’, and points out that they are frictional, but not in the classic sense of a Coulomb model involving dilation and frictional sliding between grains (Campbell, 2006). Rather, motion involves the continuous buildup and collapse of granular force chains (see, e.g., Howell *et al.*, 1999; Campbell, 2005, 2006; Mair and Hazzard, 2007). In the absence of external excitation (in this case, vibrations), gravitational energy is converted to a mean shearing motion wherein velocity gradients contribute to fluctuating grain motions that are dissipated via inelastic collisions (Campbell, 1990). What is particularly interesting about the flows in the RR experiments is the added effect of the externally derived excitation. In addition to being a second source of fluctuating grain motions, an effect of this excitation is to contribute to the disruption of force chains (Campbell, 2003; Hostler and Brennen, 2005a, 2005b), which in turn contributes to the gravity driven shearing motion in these experiments.

The point of this contribution is to describe how force-chain effects enter this problem, and give rise to the exponential-like profiles of grain displacement in the RR experiments. Our analysis below appeals to a simple idea. The forces resisting grain motion derive from force chains. Such chains are disrupted by both shearing motions and vibrations. But force chains are also generated by shearing motion. The geometry of the collective grain motion thus reflects a balance between the rate of production and the rate of disruption of force chains. Although the formulation

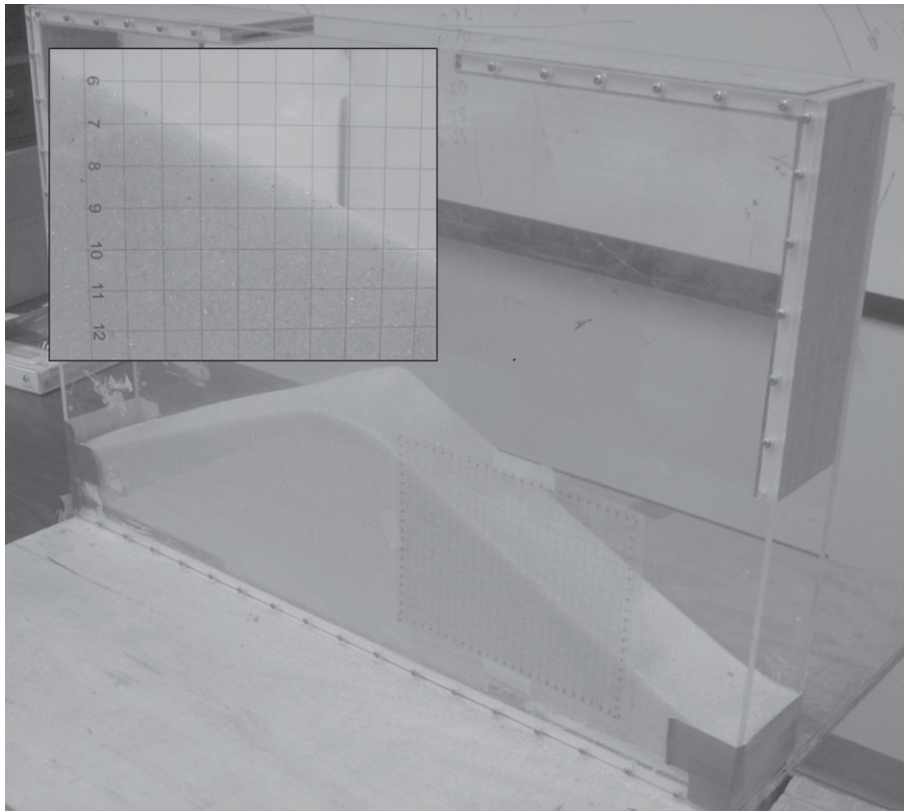


**Figure 1.** Image of experimental acrylic box containing sloping granular material, and centimeter-ruled measurement grid (inset); the box is vibrated by a sub-woofer (not shown) fixed beneath it.

is specifically aimed at the RR experiments, the results lend special value to these one-of-a-kind experiments in that they reveal ingredients of the basic behavior of granular flows in a broader context.

We note that, in aiming at parsimony, the analysis appeals to simple geometrical and mechanical scaling. Algebraic expressions in the formulation therefore do not include numerical factors. This means that, although functional forms for the grain speed and flux are dimensionally sound, certain quantities within them cannot be numerically constrained, so the comparison of the formulation with the data from the RR experiments remains at a qualitative level.

## Ingredients of Motion

### Grain excitation

The grains in the RR experiments undergo excitation due to vertical accelerations of the acrylic box (Figure 1). These accelerations derive from vibrations of an acoustic speaker (sub-woofer) fixed to the bottom of the box. The speaker, driven by a white-noise source, passes this noise to a sub-woofer frequency range of  $\sim 20$ – $200$  Hz. The geometry and mass of the speaker–box–grain system, and the coupled motions of these system components – as a massive, dissipative system – then pass this sub-woofer range of frequencies to lower frequencies of vertical vibrations.

The sidewalls of the box, with finite rigidity, experience flexural vibrations as they interact with the granular material between them. The intensity of such sidewall vibrations must vary horizontally due to the finite breadth of the sidewalls and vertically due to the finite height of the sidewalls with fixed base and free top, and due to the coupling between the sidewalls and the granular material filling the lower part of the box, notably involving a sharp transition in this coupling across the free surface of the granular material.

Grains ‘deep’ within the granular material may or may not lose contact with the base or sidewalls depending on the magnitude of the boundary accelerations and the overburden stress. With sufficiently large boundary accelerations,

grains may lose contact with the boundaries and therefore experience collisions with them. If, with sufficient overburden (probably involving a depth of at least several hundred grain diameters (see, e.g., Potapov and Campbell, 1996)), the grains deform elastically over the full amplitude of the boundary vibrations, then the grains can maintain contact with the boundaries. Grains close to, or at, the surface of the granular material are more likely to experience a loss of contact with the sidewalls and therefore undergo collisions with them.

## Granular temperature

Let  $x$  denote a horizontal coordinate that is parallel to the box sidewall and positive in the downslope direction, let  $y$  denote a horizontal coordinate that is normal to  $x$  and let  $z$  denote a vertical coordinate with origin ( $z = 0$ ) positioned at the base of the box (Figure 1). Moreover, letting  $\mathbf{u} = \mathbf{i}u + \mathbf{j}v + \mathbf{k}w$  denote the grain velocity, then  $\mathbf{u} = \mathbf{u}_m + \mathbf{u}'$ , where  $\mathbf{u}_m$  is the velocity of the (ensemble) mean motion and  $\mathbf{u}'$  is the fluctuating grain velocity.

Inasmuch as vibrations of the box in the RR experiments contribute to differential grain motions, such grains possess a finite granular temperature  $T$ . Production of granular temperature also occurs with the shearing motion of the near-surface layer in these experiments. The granular temperature is defined as

$$T = \frac{1}{3} |\langle \mathbf{u}'^2 \rangle| = \frac{1}{3} (\langle u'^2 \rangle + \langle v'^2 \rangle + \langle w'^2 \rangle) \quad (1)$$

and is generated from two sources: collisional production and streaming production. Production of granular temperature by streaming is only important in the presence of a velocity gradient in the mean motion. This mechanism of production is analogous to the generation of fluctuating speeds in kinetic theory, as grains move from an area of high mean velocity and on average carry this velocity into an area of low mean velocity, or vice versa, before interacting with other grains. Production by collisions also occurs in relation to such velocity gradients, but does not require them. Focusing first on this latter source of granular temperature, physical and numerical experiments that excite a granular layer from below deserve notice for comparison with the RR experiments.

In experiments (e.g. Yang *et al.*, 2002), the solid base beneath a granular layer is accelerated vertically as a low-amplitude high-frequency sinusoid, independently of grain motions above. In analogous numerical experiments (e.g. Ramírez and Soto, 2003), the excitation at the base is steady, where rebounding grain speeds are sorted as a Maxwellian distribution. In these experiments, grains are brought to a steady state in their macroscopic quantities averaged horizontally. Moreover, no mean motion, and therefore no velocity gradients, exist. Notably, then, the granular density  $n$  (number of grains per unit volume) involves an inversion: it is low near the base, increases to a maximum value at finite distance from the base, then declines upward to the free surface. In turn, the granular temperature is high at the base, declines to a minimum value at finite distance, then increases upward. The significance of these experiments is that they demonstrate how the granular heat flux  $\mathbf{J}$  for inelastic grains satisfies the generalized law (see, e.g., de Groot and Mazur, 1984)

$$\mathbf{J} = -k_T \nabla T - \mu \nabla n \quad (2)$$

where  $k_T$  is a thermal conductivity and  $\mu$  is a transport coefficient that vanishes for elastic systems (Lun *et al.*, 1984; Brey *et al.*, 1996, 1998; Dufty *et al.*, 1997; Garzó and Dufty, 1998). These experimental systems are in a conducting state (e.g. not involving convection, grain clustering or oscillating behavior), and thus a steady flux  $\mathbf{J}$  is conducted to the free surface despite an adverse temperature gradient in the upper part of the granular fluid. Interestingly, the granular temperature increases with vanishing grain concentration above the free surface in these experiments. A lovely explanation of this is provided by Campbell (2006).

In contrast to these low-concentration experiments, where granular concentrations can locally be significantly less than the close-packing concentration, deep-layer high-concentration experiments (e.g. Potapov and Campbell, 1996; Hostler and Brennen, 2005a, 2005b) also deserve notice. In such experiments the concentration remains close to the close-packing concentration and the oscillating lower boundary induces elastic waves that propagate upward through the granular layer. These waves generate a granular temperature manifest as oscillating grain motions with wave passage. With sufficient overburden the grains deform elastically over the full amplitude of the boundary oscillations, and the grains maintain contact with the boundary despite accelerations in excess of  $g$  (Potapov and Campbell, 1996).

The RR experiments are like these experiments in that grains are excited by boundary oscillations. At depth, inasmuch as grains maintain contact with the base and sidewalls, then like the experiments of Potapov and Campbell (1996) and Hostler and Brennen (2005b) grain excitation occurs via elastic waves. These experiments differ from the RR experiments in that the granular concentrations are significantly lower (in the experiments of Yang *et al.* (2002) and Ramírez and Soto (2003)), the boundary oscillations are independent of the grain behavior, and the granular

density and temperature vary in only one dimension. Moreover, the RR experiments probably involve transient rather than steady granular temperature and density fields.

Granular temperature is also produced by collisional and streaming mechanisms during the shearing motion of the grains (e.g. Campbell, 2006). The collisional mechanism generally dominates at large grain concentrations, and is probably dominant in the RR experiments except possibly at the free surface. Moreover, unlike the thermodynamic temperature, the granular temperature is not necessarily isotropic. (The physical experiments of Yang *et al.* (2002) with mustard seeds nicely illustrate this point.) In shear flows, that part of the granular temperature composed of the fluctuating speeds measured parallel to the mean motion is generally greater than that part involving fluctuating speeds measured parallel to the velocity gradient. This anisotropy increases with decreasing grain concentration as the relative importance of the streaming mechanism increases, but with large concentration where the collisional mechanism is dominant the granular temperature becomes nearly isotropic (Campbell, 1989).

That the grains in the RR experiments are raised to a finite granular temperature is directly evidenced by the dispersion of tracer grains in the experiments of Roering (2004, Figures 5 and 6). Indeed, the granular temperature is a direct measure of relative motions among grains. It is also evident in these experiments that the amount of dispersion, and inferably the granular temperature, increases toward the free surface. The tracers further suggest increasing anisotropy toward the surface, and this may partly reflect that surface (and near surface) tracers experienced significant streaming during the shearing motion.

### Force chains

To move downslope, the excited near-surface layer in the RR experiments must be diluted to allow differential grain motions, and the granular concentration is likely close to the so-called critical concentration  $c_c$ . When excitation ceases, layer motion ceases (although grains previously launched from the surface continue to bounce around). Thus, although it may be roughly correct that grains maintain constant frictional contact with their neighbours (Roering, 2004, p. 1604), this represents an incomplete image of friction during the shearing motion. Certainly the collective motion includes differential sliding of grains one against another, an ingredient of dissipation of granular energy to heat, but the collective motion almost certainly includes momentary weakening, if not separation, albeit mostly small, of grain contacts that leads to disruption of force chains (Figure 2). Several items point to this. The source of collective motion is gravitational only upon excitation. Qualitatively, this onset of motion is like lowering the internal friction angle, momentarily allowing failure at a slope that is less than the nominal static critical angle. Gravity alone cannot provide this weakening and initiation of motion. Rather, this behavior must involve initial disruption of the static force-chain network with excitation, giving a force imbalance that initiates motion. This disruption, in turn, requires a finite granular temperature. Indeed, the launching of surface grains, representing large grain separations, illustrates locally high granular temperatures. With cessation of vibration, motion ceases. That is, a force-chain network that supports the static stress field is reestablished, as before the onset of vibration.

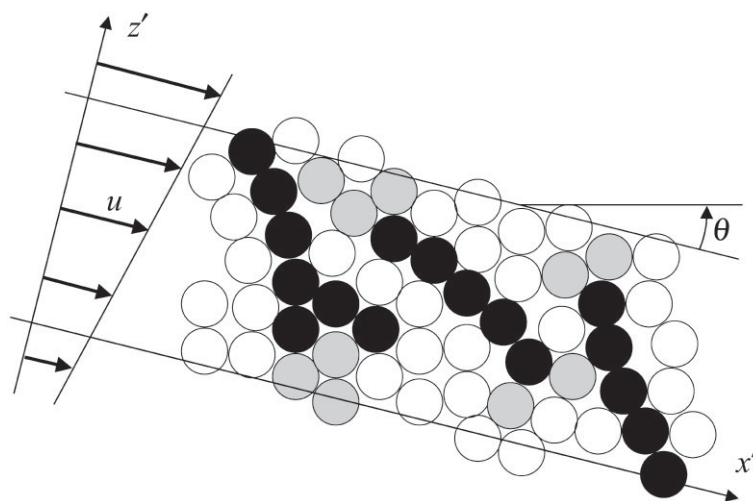


**Figure 2.** Idealized granular shear flow with inclined  $x'$ - $z'$  coordinate system showing force-chain participants (black), other force-bearing grains (grey) and spectators (white); modified from Cates *et al.* (1998).

Resistance to granular motion in the RR experiments is provided by force chains (Figure 2). For a surface parallel to shearing motion, conservation of the number of force chains per unit area  $N$  [number  $L^{-2}$ ] requires a balance between the production and destruction of chains:

$$\frac{dN}{dt} = P - Q_\gamma - Q_f - Q_T. \quad (3)$$

Production is represented by the term  $P$  [number  $L^{-2} t^{-1}$ ]. Destruction involves three mechanisms represented by  $Q_\gamma$ ,  $Q_f$  and  $Q_T$  [number  $L^{-2} t^{-1}$ ]. As described further below,  $Q_\gamma$  describes force-chain destruction associated with shearing motion,  $Q_f$  describes destruction associated with vibrations and  $Q_T$  describes destruction associated with grain collisions. Under steady motion  $dN/dt = 0$  and  $P = Q_\gamma + Q_f + Q_T$ .

At a particular concentration  $c$  per unit area the rate of production of force chains  $P$  goes with the rate of shear, namely  $P \sim \alpha\gamma$ , where  $\alpha$  [number  $L^{-2}$ ] is a factor and the shear rate  $\gamma = du/dz$  [ $t^{-1}$ ]. This production of chains is purely geometrical in relation to shearing motion, and is therefore independent of the gravitational field.

Shear also leads to chain destruction. Specifically, the rate of chain destruction  $Q_\gamma$  goes with the shear rate and with the number of extant chains, namely  $Q_\gamma \sim \alpha_\gamma\gamma N$ , where  $\alpha_\gamma$  is a dimensionless factor. This describes the ‘aging’ of chains during rotation, whence they become unstable and self-destruct (Campbell, 2006). As described below, the factor  $\alpha_\gamma$  may weakly depend on the flow geometry in relation to the gravitational field.

Momentarily neglecting  $Q_f$  and  $Q_T$  (described next), under steady motion  $P = Q_\gamma$  in which case  $\alpha = \alpha_\gamma N$ . Moreover, by definition, the chain longevity  $t_1$  [t] during steady shear is  $t_1 = N/P \sim N/\alpha\gamma \sim 1/\alpha_\gamma\gamma$ . The instantaneous number of chains per unit area  $N \sim Pt_1 \sim Q_\gamma t_1 \sim \alpha/\alpha_\gamma$  is therefore independent of the shear rate  $\gamma$  (Campbell, 2006).

Disruption of force chains also occurs when the acceleration of a vibration with amplitude  $A$  and frequency  $f$  is sufficient to break chain ‘links’, either by separating grains in a chain, or by weakening grain–grain contacts such that chain–grain interactions break force-chain links during shear. The possible number of chain disruptions per unit time goes with  $f$ , of which only some proportion  $\beta$  occurs. That is, this rate can be no greater than  $f$  ( $\beta = 1$ ), and the longevity of chains subject to such vibrations (in absence of shear) can be no shorter than  $1/f$ . Thus the longevity associated with vibrations goes as  $1/\beta f$ , and it is assumed that  $Q_f \sim \beta f N$ . (The factor  $\beta$  is examined further below.)

The term  $Q_T$  in (3) describes destruction of force chains in relation to grain–chain collisions, inasmuch as chains are weakened by collisions with surrounding grains. As described below, this term becomes significant only with avalanching (and relatively high granular temperature) when the surface slope exceeds a critical value. It is assumed that  $Q_T \sim \varepsilon N$ , where the factor  $\varepsilon$  [ $t^{-1}$ ] is like the reciprocal of the mean free time.

Collecting production and destruction terms, the force-chain longevity is

$$t_1 \sim \frac{N}{\alpha\gamma} \sim \frac{1}{\alpha_\gamma\gamma + \beta f + \varepsilon}. \quad (4)$$

In turn, the number of chains per unit area is

$$N \sim \frac{\alpha\gamma}{\alpha_\gamma\gamma + \beta f + \varepsilon}. \quad (5)$$

Over an area  $B$  the force  $F$  associated with chains is  $F \sim k\delta NB$ , where  $k$  is the grain-contact stiffness and  $\delta$  is the grain-to-grain deformation. In turn the stress  $\tau \sim F/B \sim k\delta N$ , so

$$\tau \sim \frac{F}{B} \sim k\delta \frac{\alpha\gamma}{\alpha_\gamma\gamma + \beta f + \varepsilon}. \quad (6)$$

This says that in the absence of vibrations ( $f = 0$ ) and free failure ( $\varepsilon = 0$ ), the stress  $\tau$  is independent of the shear rate as implied by the scaling above. This result is equivalent to saying that, like fixed volume experiments, the stress is independent of the shear rate in the elastic–quasi-static regime (Campbell, 2006). On the other hand, (6) suggests that, for a given magnitude of  $\tau$  determined by the geometry of the granular flow and a given depth within it, then with  $f > 0$  or  $\varepsilon > 0$  the shear rate  $\gamma$  must increase to satisfy  $\tau$ . That is, with an increasing rate of destruction of force chains by vibrations or collisions, then such chains must be produced more rapidly by an increasing shear to sustain the number of chains (and  $\tau$ ). Indeed, the onset of motion in the RR experiments marks the initial disruption of static chains and a force imbalance leading to ‘failure’ and shearing motion. This motion in turn produces new chains that dynamically balance the driving forces.

### Velocity Profiles and Grain Flux

#### Constant grain stiffness

The factors  $\alpha_\gamma$ ,  $\beta$  and  $\varepsilon$  are key ingredients in (6). To clarify their meaning, consider an inclined coordinate system (Figure 2):  $x'$  is parallel to the granular surface and positive downslope, and  $z'$  is normal to  $x'$  and positive upward. Then the depth  $h = -z'$  with origin ( $h = 0$ ) at the surface. Now, with  $\gamma = du/dz' = -du/dh$ , (6) may be rearranged to

$$\frac{du}{dh} \sim \frac{\beta f + \varepsilon}{\alpha_\gamma - \alpha \frac{k\delta}{\tau}} \tag{7}$$

For  $\varepsilon = 0$  (elastic–quasi-static flow without free failure), shear occurs only with vibration ( $f > 0$ ). In the absence of vibrations ( $f = 0$ ), the surface slope  $S$  must be above a critical value  $S_c$  for finite shear, such that  $\varepsilon > 0$ . With  $f > 0$  or  $\varepsilon > 0$ , the denominator cannot vanish, as  $du/dh$  must remain finite. With these points in mind, let us start with  $\beta$ .

The disruption of a force chain involving separation of grains occurs when the amplitude  $A$  of grain–grain deformation  $\delta$  associated with elastic waves exceeds the magnitude of the static deformation  $\delta_s$  (Campbell, 2003). The disruption of a chain also occurs with vibrations of neighboring grains. The likelihood of this increases with  $A$ . (Note that the disruption of a force chain in a granular medium does not require separation of its grains, just sufficient reduction in the force holding the chain together as it interacts with surrounding grains during shear (Campbell, 2003).) Both  $A$  and  $\delta_s$  vary locally, as the propagation of elastic waves (speed and intensity) depends on the granular concentration, specifically the coordination number (the number of contacts between a grain and its neighbors), which varies with overburden (Potapov and Campbell, 1996; Hostler and Brennen, 2005a, 2005b). To first order it is thus assumed that the factor  $\beta \sim A/\delta_s$ . That is, when the wave amplitude  $A \rightarrow 0$  the likelihood of chain disruption due to vibrations vanishes, and as  $A$  approaches the local static deformation  $\delta_s$  the likelihood of disruption increases.

With grain density  $\rho_s$  the normal overburden stress on planes normal to  $z'$  goes as  $\rho_s c g \cos \theta h$ . In turn, it is assumed that  $k\delta \sim k\delta_s \sim \rho_s c g \cos \theta h / N_g$  or that  $\delta_s \sim \rho_s c g \cos \theta h / k N_g$ . Here, the number of grains per unit area  $N_g \sim 1/d^2$ , where  $d$  is a characteristic grain diameter. In this approximation the deformation  $\delta$  is assumed to be sufficiently small that the stiffness  $k$  is essentially constant and independent of  $\delta$  (Potapov and Campbell, 1996; Campbell, 2006). The theory of Hertz (1882) suggests that for spherical grains  $k \sim \delta^{1/2}$ , although experimental evidence suggests that at low overburden pressures  $k \sim \delta$  (Campbell, 2006), giving a grain contact force  $F_g \sim k_0 \delta^2$ . (This point is considered in the next section.)

At depth  $h$  the stress that must be supported by force chains is  $\tau = \rho_s c \sin \theta h$ . The force balance requires that  $\tau \sim k\delta \cos \phi N$ , where  $\phi$  is the typical angle of force chains relative to a surface parallel to shearing motion. Using (6) this gives

$$\rho_s c g \sin \theta h \sim \frac{\cos \phi}{N_g} \rho_s c g \cos \theta h - \frac{\alpha \gamma}{\alpha_\gamma \gamma + \frac{N_g k A f}{\rho_s c g \cos \theta h} + \varepsilon} \tag{8}$$

With  $\gamma = du/dz' = -du/dh$  and  $S = \tan \theta$ , this becomes

$$\frac{du}{dh} \sim \frac{S}{\left(1 - \frac{\alpha_\gamma}{\alpha \cos \phi d^2} S\right) \cos \theta} \frac{A k f}{\alpha \cos \phi \rho_s c g d^4 h} - \frac{S}{1 - \frac{\alpha_\gamma}{\alpha \cos \phi d^2} S} \frac{\varepsilon}{\alpha \cos \phi d^2} \tag{9}$$

The ratio  $\alpha_\gamma / \alpha d^2 \sim (N_g / N) / (1 + \beta f / \alpha_\gamma \gamma + \varepsilon / \alpha_\gamma \gamma)$  is a measure of the number of grains per unit area to the number of force chains per unit area; thus  $\alpha_\gamma / \alpha \cos \phi d^2 > 1$ . One may think of this as the number of grains/chains intersecting a surface that is parallel to the shearing motion, per unit area of this surface. Furthermore, finite shear requires that  $\alpha_\gamma S / \alpha \cos \phi d^2 < 1$ ; thus  $1 < \alpha_\gamma / \alpha \cos \phi d^2 < 1/S$ . Setting  $S$  to its critical value  $S_c$  implies that  $1 < \alpha_\gamma / \alpha \cos \phi d^2 \leq 1.5$ , suggesting that many grains actively participate as members of chains, rather than as spectators (Figure 2), as  $S \rightarrow S_c$ .

Turning to the quantity  $\varepsilon$ , this is likely to be a complex function of grain motion and depth. Inasmuch as it represents destruction of force chains by collisions, it can only be significant at relatively high flow rates and granular temperature (within the elastic–inertial regime of Campbell (2005, 2006)). It is thus assumed that  $\varepsilon \sim \varepsilon_T T^{1/2}$ , where  $\varepsilon_T [L^{-1}]$  is like the reciprocal of the mean free path. In turn,  $T^{1/2} \sim u$ , so  $\varepsilon \sim \varepsilon_T u$ , which suggests that this term is mostly important near the grain-flow surface. In the next few steps, this term is neglected. The approximation therefore pertains to the domain of  $S < S_c$  in the presence of vibrations.

Neglecting the term in (9) involving  $\varepsilon$ , a solution of (9) is

$$\frac{u}{u_0} = 1 - \ln\left(\frac{h}{h_0}\right) \quad (10)$$

where  $u_0 = u(h_0)$  is the depth-averaged velocity, namely

$$u_0 = \frac{S}{\left(1 - \frac{\alpha_\gamma}{\alpha \cos \phi d^2} S\right) \cos \theta} \frac{A k f}{\alpha \cos \phi \rho_s c g d^4}. \quad (11)$$

Note that  $h_0 = H/e$ , where  $H$  is the depth at which  $u = 0$ .

If we momentarily neglect the uppermost data in the six grain-speed profiles in Figure 7 of Roering (2004), with the idea that motion of the top layer (a few grain diameters) probably involves streaming behavior and possibly ingredients of saltation, then simple regression yields direct estimates of  $u_0$  and  $h_0$ , whence the data collapse to a single line consistent with the form of (10) (Figure 3). We note that estimates of  $u_0$  using these regressions are systematically less than estimates of  $u_0$  based on numerical integrations (Riemann sums) that include the uppermost data.

The regressions above retrieve estimates of the depth  $H$  for each of the six profiles independently. If on physical grounds we instead insist that the value of  $H$  ought to be the same for a given vibration intensity – with the idea that  $H$  is set by the overburden at which force-chain disruption by vibrations becomes negligible, independently of slope – then alternatively we may write (10) as  $u \sim [SI/(1 - N^*S) \cos \theta] \ln(h/H)$ , where  $N^* = \alpha_\gamma/\alpha \cos \phi d^2$ , and  $I$  denotes the ratio in (11) involving  $A$ . The quantity  $I$  is a measure of the vibration intensity. Upon rearranging this to  $u^* = u/(1 - N^*S) \cos \theta/SI \sim \ln(h/H)$ , and choosing values of the quantities  $N^*$ ,  $I$  and  $H$  that provide a good visual fit, the data for three values of slope  $S$  and two intensities  $I$  (Figure 7, Roering, 2004) again collapse to a single line (Figure 4). The import of this is that a reasonable qualitative fit is obtained with the same values of  $H$  and  $N^*$  for each vibration intensity, that the two estimates of  $H$  (0.12 and 0.13 m for low and high intensities, respectively) and of  $I$  (0.003 and 0.004 m s<sup>-1</sup> for low and high intensities, respectively) are physically consistent, and that, most notably, the two estimates of  $N^* = \alpha_\gamma/\alpha \cos \phi d^2$  (1.6 and 1.8 for low and high intensities, respectively) are entirely consistent with the scaling presented above for  $S < S_c$ .

Turning to the grain flux per unit width  $q$  (Roering, 2004, Figure 8), by definition  $q = Hu_0$ . In turn, the depth  $H \sim H_0/\cos \theta$ , where  $H_0$  is the overburden depth at which disruption of force chains by vibrations effectively ceases beneath a horizontal surface. Then,

$$q \sim \frac{H_0 S}{\left(1 - \frac{\alpha_\gamma}{\alpha \cos \phi d^2} S\right) \cos^2 \theta} \frac{A k f}{\alpha \cos \phi \rho_s c g d^4}. \quad (12)$$

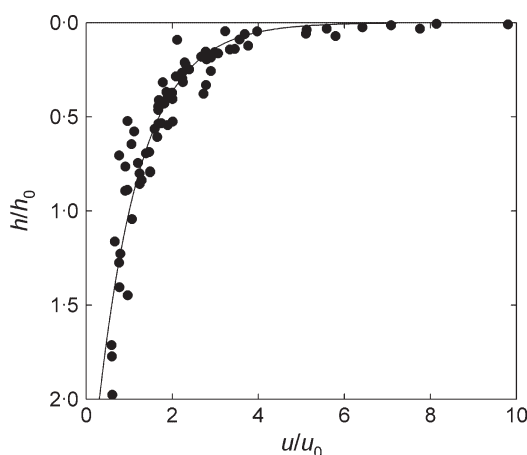


**Figure 3.** Plot of dimensionless grain speed  $u/u_0$  versus dimensionless depth  $h/h_0$  using data from Figure 7 of Roering (2004) involving slopes of 15, 20 and 25° under low intensity and high intensity vibrations.

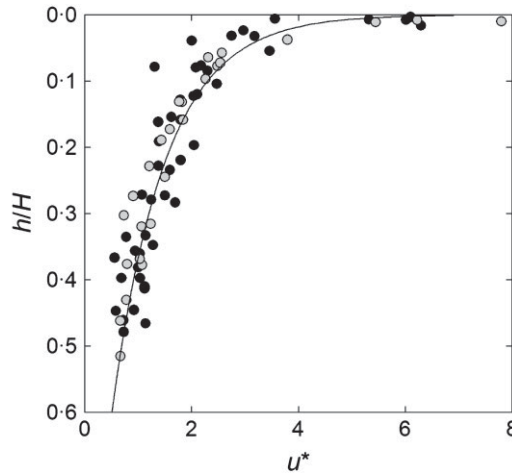


**Figure 4.** Plot of dimensionless grain speed  $u^*$  versus dimensionless depth  $h/H$  using data from Figure 7 of Roering (2004) for slopes of 15, 20 and 25° under low intensity (black) and high intensity (grey) vibrations based on  $N^* = 1.6$ ,  $I = 0.003 \text{ m s}^{-1}$  and  $H = 0.12 \text{ m}$  (black) and  $N^* = 1.8$ ,  $I = 0.004 \text{ m s}^{-1}$  and  $H = 0.13 \text{ m}$  (grey); the increase in  $N^*$  and  $H$  with  $I$  is physically consistent.

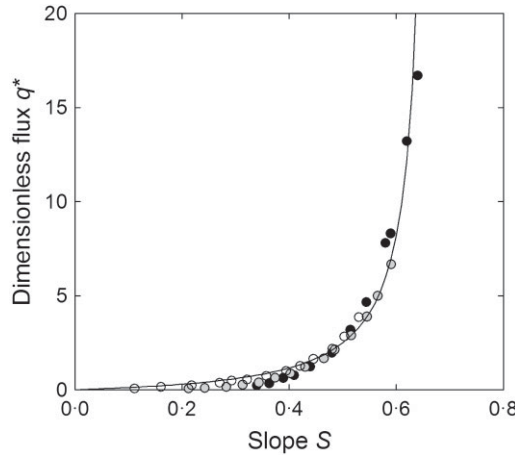


**Figure 5.** Plot of dimensionless grain flux  $q^* = q/I_0$  versus slope  $S$  using data from Figure 8 of Roering (2004) for low (black), medium (grey) and high (white) intensity vibrations, scaled by reported ratio of 1:3:5, namely, medium intensity data are divided by three and high intensity data are divided by five; theoretical curve (solid line) is based on the parametric values  $N^* = 1.5$  and  $I_0 = 0.1 \text{ cm}^2 \text{ s}^{-1}$ .

This yields a strongly nonlinear increase in  $q$  with slope  $S$ . Used in a curve-fitting mode this looks like  $q \sim SI_0 / (1 - N^*S) \cos^2\theta$ , where  $I_0 = H_0I$ . Upon rearranging this to  $q^* = q/I_0 \sim S / (1 - N^*S) \cos^2\theta$ , data for three intensities from Figure 8 of Roering (2004) collapse to a single line when the intensities are scaled by the reported factor of 1:3:5 (Figure 5). The rate of increase in  $q^*$ , and the domain of  $S$  over which  $q^*$  rapidly approaches infinity, are sensitive to the ratio  $N^* = \alpha_\gamma / \alpha \cos \phi d^2$  (the ratio of the number of grains to the number of chains per unit area, modulated by the force-chain orientation  $\cos \phi$ ). The estimated value of  $N^* = 1.5$  is consistent with the scaling presented above.

### Strain-dependent stiffness

If it is assumed that  $k \sim \delta$  or  $k \sim \delta^{1/2}$  (i.e. Hertzian), then (6) looks like

$$\tau \sim k_0 \delta^n \frac{\alpha \gamma}{\alpha_\gamma \gamma + \beta f + \varepsilon} \tag{13}$$

with  $n = 2(k \sim \delta)$  or  $n = 3/2(k \sim \delta^{1/2})$  and  $\delta_s \sim (\rho_s c g d^2 \cos \theta h / k_0)^{1/n}$ . In turn, neglecting  $\varepsilon$ , (11) looks like

$$u \sim \frac{S}{\left(1 - \frac{\alpha_\gamma}{\alpha \cos \phi d^2} S\right) \cos^{1/n} \theta} \frac{Ak_0^{1/n} f}{(1 - 1/n)\alpha \cos \phi d^2 (\rho_s c g d^2)^{1/n}} (H^{1-1/n} - h^{1-1/n}). \quad (14)$$

The form of this for both  $n = 2$  and  $n = 3/2$  can be fitted to the profiles in Figure 7 of Roering (2004), although it typically underestimates the datum nearest the surface in each plot.

### Higher-order effects

The approximations herein have assumed that the granular concentration  $c$  is constant (and approximately equal to the critical concentration  $c_c$ ). It must be noted, however, that small variations in  $c$ , which most certainly exist over the thickness of the granular material in the RR experiments, can have important effects. These include influences on the strength of force chains and the propagation of elastic waves (Hostler and Brennen, 2005a, 2005b). Such variations in  $c$  can also reflect small variations in granular temperature, and the possibility of behavior in the elastic–inertial regime (Campbell, 2006) at high flow rates. This case requires a different force balance wherein force chains must also accommodate grain/chain inertia during shear (Campbell, 2004, 2005).

The factor  $\alpha_\gamma$  may weakly depend on the flow geometry in relation to the gravitational field. Recall that this factor describes destruction of force chains in relation to their ‘aging’ during rotation. Part of this destruction probably involves the orientation of chains relative to the gravitational field. Namely, at large slope  $S$ , chains under the influence of gravity may collapse sooner than they might otherwise at a lower slope.

We finally note that the static version of (8) provides an interesting interpretation of the critical slope  $S_c$ . Namely, setting  $f$  and  $\varepsilon$  in (8) to zero and assuming a critical state,

$$S_c \sim \frac{\alpha \cos \phi}{\alpha_\gamma N_g} \approx \frac{N}{N_g} \cos \phi. \quad (15)$$

Comparing this with (5), the number of force chains per unit area  $N$  is at its maximum value. Vibrations decrease this value, which is equivalent to lowering the critical slope.

## Conclusions

The essential point of this analysis is embodied in the statement of conservation (3) and in the force balance (6). Inasmuch as force chains provide resistance to grain motion, then the geometry of the motion is determined by a dynamic balance between the production and destruction of force chains. An increasing rate of destruction of force chains by vibrations or collisions requires an increasing rate of production by shear to maintain this balance. The analysis is consistent with the exponential-like profiles of grain displacement, and the strongly nonlinear increase in grain flux with increasing surface slope, observed in the RR experiments. The analysis also suggests that the critical slope is set by the ratio of the number of force chains to the number of grains per unit area, modulated by the force-chain orientation.

## Acknowledgements

Peter Haff talked us through certain subtleties of granular temperature. We thank Peter and an anonymous reviewer for helping us focus our presentation. This work was supported in part by the National Science Foundation (EAR-0405119).

## References

- Brey JJ, Dufty JW, Kim CS, Santos A. 1998. Hydrodynamics for granular flow at low density. *Physical Review E* **58**: 4638–4653.
- Brey JJ, Moreno F, Dufty JW. 1996. Model kinetic equation for low-density granular flow. *Physical Review E* **54**: 445–456.
- Campbell CS. 1989. The stress tensor for simple shear flows of a granular material. *Journal of Fluid Mechanics* **203**: 449–473.
- Campbell CS. 1990. Rapid granular flows. *Annual Reviews of Fluid Mechanics* **22**: 57–92.
- Campbell CS. 2002. Granular shear flows at the elastic limit. *Journal of Fluid Mechanics* **465**: 261–291.
- Campbell CS. 2003. A problem related to the stability of force chains. *Granular Matter* **5**: 129–134.
- Campbell CS. 2004. Elastic granular flows. *International Journal of Chemical Reactor Engineering* **2**: 2.
- Campbell CS. 2005. Stress controlled elastic granular shear flows. *Journal of Fluid Mechanics* **539**: 273–297.

- Campbell CS. 2006. Granular material flows – an overview. *Powder Technology* **162**: 208–229.
- Cates ME, Wittmer JP, Bouchaud J-P, Claudin P. 1998. Jamming, force chains, and fragile matter. *Physical Review Letters* **81**: 1841–1844.
- de Groot SR, Mazur P. 1984. *Non-Equilibrium Thermodynamics*. Dover: New York.
- Dufty JW, Brey JJ, Santos A. 1997. Kinetic models for hard sphere dynamics. *Physica A* **240**: 212–220.
- Garzó V, Dufty JW. 1998. Dense fluid transport for inelastic hard spheres. *Physical Review E* **59**: 5895–5910.
- Hascoët E, Herrmann HJ, Loreta V. 1999. Shock propagation in a granular chain. *Physical Review E* **59**: 3202–3206.
- Hertz H. 1882. Über die Berührung fester elastischer Körper. *Journal für die Reine und Angewandte Mathematik* **92**: 156–171.
- Hostler SR, Brennen CE. 2005a. Pressure wave propagation in a granular bed. *Physical Review E* **72**: 031303.
- Hostler SR, Brennen CE. 2005b. Pressure wave propagation in a shaken granular bed. *Physical Review E* **72**: 031304.
- Howell DW, Behringer RP, Veje CT. 1999. Stress fluctuations in a 2D granular Couette experiment: a continuous transition. *Physical Review Letters* **26**: 5241–5244.
- Lun CKK, Savage SB, Jeffrey DJ, Chepurny N. 1984. Kinetic theories for granular flow: inelastic particles in Couette flow and slightly inelastic particles in a general flowfield. *Journal of Fluid Mechanics* **140**: 223–256.
- Mair K, Hazzard JF. 2007. Nature of stress accommodation in sheared granular material: insights from 3D numerical modeling. *Earth and Planetary Science Letters* **259**: 469–485.
- Potapov AV, Campbell CS. 1996. Propagation of elastic waves in deep vertically shaken particle beds. *Physical Review Letters* **77**: 4760–4763.
- Ramírez R, Soto R. 2003. Temperature inversion in granular fluids under gravity. *Physica A* **322**: 73–80.
- Roering JJ. 2004. Soil creep and convex-upward velocity profiles: theoretical and experimental investigation of disturbance-driven sediment transport on hillslopes. *Earth Surface Processes and Landforms* **29**: 1597–1612.
- Roering JJ, Kirchner JW, Sklar LS, Dietrich WE. 2001. Hillslope evolution by nonlinear creep and landsliding: an experimental study. *Geology* **29**: 143–146.
- Yang X, Huan C, Candela D, Mair RW, Walsworth RL. 2002. Measurements of grain motion in a dense, three-dimensional granular fluid. *Physical Review Letters* **88**. DOI: 10.1103/PhysRevLett.88.044301